Polyhedron 85 (2015) 926–932

Contents lists available at ScienceDirect

Polyhedron

journal homepage: www.elsevier.com/locate/poly

Heteroleptic ruthenium(II) complexes of 2-(2-pyridyl)benzimidazoles: A study of catalytic efficiency towards transfer hydrogenation of acetophenone

Osman Dayan [a,*], Selin Demirmen [a], Namık Özdemir [b]

[a] Çanakkale Onsekiz Mart University, Department of Chemistry, Laboratory of Inorganic Synthesis and Molecular Catalysis, 17020 Çanakkale, Turkey
[b] Department of Physics, Faculty of Arts and Sciences, Ondokuz Mayıs University, 55139 Samsun, Turkey

ARTICLE INFO

Article history:
Received 26 August 2014
Accepted 15 October 2014
Available online 24 October 2014

Keywords:
Ru(II) complexes
Transfer hydrogenation
Benzimidazoles
Acetophenone
Pyridines

ABSTRACT

Six ruthenium(II) complexes ([$RuCl_2$(*p*-cymene)(**L1–6**)], **SD1–6**, (**L1–6**: bidentate pyridyl-benzimidazole ligands)) were synthesized from [$RuCl_2$(*p*-cymene)]$_2$ dimer and bidentate pyridyl-benzimidazole ligands. The compounds were characterized by elemental analysis, IR, UV–Vis, NMR and X-ray diffraction. The synthesized Ru(II) complexes (**SD1–6**) were tested as catalysts for the catalytic transfer hydrogenation (CTH) of acetophenone to secondary alcohols in the presence of KOH using 2-propanol as a hydrogen source at 82 °C. All complexes were active catalysts for TH of acetophenone with good yields under mild conditions (after 15 min, yields of up to 91%).

1. Introduction

Nitrogenous donor multidentate ligands are very attractive in coordination chemistry because of their simplicity and availability [1]. The steric and electronic properties around metal center easily changed with these ligands. By the way, catalytically active metal complexes having special properties have been synthesized. One of those type ligands is a pyridine based bidentate ligand 2-(pyridin-2-yl)-1H-benzimidazoles. This chelator ligand can be easily derivatized and strongly bind metal center.

On the other hand, the chemistry of ruthenium plays an important role in many applications [2–9]. For example, Ru(II)-pyridyl complexes has been attention due to potential applications in the field of optoelectronic devices, medicinal chemistry, catalysis, etc. [10–18]. Success depends on complex geometries and ligand modification in these applications.

Because of easy working and relatively low cost, catalytic transfer hydrogenation (CTH) of carbonyl compounds is preferred in industrial and laboratory scale. Since discovered by Noyori, Ru(II) complexes are the most popular catalysts for the CTH [19]. Since that day, many studies show that catalytic efficiencies of complexes are directly affected by ligand properties. For this purpose, Ru(II) complexes including N-donor ligands have aimed to identify the best catalyst for CTH of carbonyl compounds [20–23]. Although there are many attempts with poly-pyridyl ligands, the catalytic studies of Ru(II) complexes bearing pyridyl-benzimidazoles was not found for CTH. In this work, we have synthesized six ionic heteroleptic Ru(II) complexes containing bidentate pyridyl-benzimidazoles and tasted as catalyst for the CTH of acetophenone. The results showed that CTH of acetophenone has achieved with good yields using simple ligands under mild conditions.

2. Experimental

The reactions were performed in air, unless otherwise stated. The reagents and solvents were obtained from commercial suppliers and used without further purification. [$RuCl_2$(*p*-cymene)]$_2$ [24] were synthesized by modification of the method in the published procedure. For other general experimental conditions, please see supporting materials.

2.1. Synthesis of compounds

2.1.1. General procedure for the ligands (*L1–6*)

L1 [25], **L2** [26], **L6** [27] were synthesized by modification of the method in the published procedure.

A solution of **L1** (0.3 g, 2.54 mmol) and KOH (0.167 g, 2.54 mmol) was refluxed for 24 h in EtOH for **L2–4** and in DMF for **L5–6**. At the end of this time, the mixture was cooled room temperature and added appropriate alkyl halide (2.54 mmol). Solution was refluxed for another 24 h. The volatiles were removed under

* Corresponding author. Tel.: +90 2862180018 1860; fax: +90 2862180533.
E-mail address: osmandayan@comu.edu.tr (O. Dayan).

http://dx.doi.org/10.1016/j.poly.2014.10.012
0277-5387/

vacuum. Residue was washed with H_2O and recrystalized with EtOH. For characterization data of **L1–6**, please see supporting materials.

2.1.2. General procedure for the synthesis of [RuCl(L)(p-cymene)]Cl, *SD1–6*

A solution of ligands (0.5 mmol) and $RuCl_2(p\text{-cymene})]_2$ (0.153 g, 0.25 mmol) was refluxed for 24 h in EtOH (10 mL). At the end of this time, the mixture was cooled room temperature and precipitated by addition of diethyl ether (30 mL). The microcrystalline solid was filtered off and washed with diethyl ether. For characterization data of **SD1–6**, please see supporting materials.

2.1.3. X-ray analysis

Intensity data of the compounds were collected on a STOE IPDS II diffractometer at room temperature (296 K) using graphite-monochromated Mo Kα radiation (λ = 0.71073 Å) by applying the ω-scan method. The structures were solved by direct methods using SHELXS-2013 [28] and refined with full-matrix least-squares calculations on F^2 using SHELXL-2013 [28] implemented in WinGX [29] program suit. All carbon bound H atoms were placed geometrically and treated using a riding model, fixing the bond lengths at 0.93, 0.98, 0.97 and 0.96 Å for aromatic CH, methine CH, CH_2 and CH_3 atoms, respectively. The hydrogen atoms of water molecules were located from a difference Fourier map and their coordinates were fixed in the final refinement. The displacement parameters

Table 1
Crystal data and structure refinement parameters for **L6** and **SD6**.

Parameter	**L6**	**SD6**
CCDC deposition No.	930498	988448
Color/shape	Light yellow/prism	Orange/prism
Chemical formula	$C_{23}H_{17}N_3$	$[RuCl(C_{10}H_{14})(C_{23}H_{17}N_3)]^+\cdot Cl^-\cdot H_2O$
Formula weight	335.39	659.59
Temperature (K)	296	296
Wavelength (Å)	0.71073 Mo Kα	0.71073 Mo Kα
Crystal system	triclinic	triclinic
Space group	$P\bar{1}$ (No. 2)	$P\bar{1}$ (No. 2)
Unit cell parameters		
a, *b*, *c* (Å)	9.7608(8), 9.9684(7), 10.4523(8)	10.3723(6), 15.2104(7), 21.7791(10)
α, β, γ (°)	78.888(6), 77.381(6), 62.798(5)	94.666(4), 101.604(4), 105.880(5)
Volume (Å^3)	877.61(12)	3203.2(3)
Z	2	4
D_{calc} (g/cm^3)	1.269	1.368
μ (mm^{-1})	0.076	0.685
Absorption correction	integration	integration
T_{min}, T_{max}	0.9562, 0.9788	0.8618, 0.9598
F(000)	352	1352
Crystal size (mm^3)	0.78 × 0.56 × 0.30	0.21 × 0.15 × 0.07
Diffractometer/measurement method	STOE IPDS II/ω scan	STOE IPDS II/ω scan
Index ranges	$-12 \leqslant h \leqslant 12$, $-12 \leqslant k \leqslant 12$, $-13 \leqslant l \leqslant 13$	$-13 \leqslant h \leqslant 13$, $-19 \leqslant k \leqslant 19$, $-27 \leqslant l \leqslant 27$
θ range for data collection (°)	$2.493 \leqslant \theta \leqslant 27.605$	$1.407 \leqslant \theta \leqslant 26.822$
Reflections collected	12 184	43 658
Independent/observed reflections	3971/3181	13 586/4714
R_{int}	0.211	0.1683
Refinement method	full-matrix least-squares on F^2	full-matrix least-squares on F^2
Data/restraints/parameters	3971/0/235	13 586/9/722
Goodness-of-fit on F^2	1.048	0.835
Final *R* indices [$I > 2\sigma(I)$]	R_1 = 0.0495, wR_2 = 0.0958	R_1 = 0.0822, wR_2 = 0.1856
R indices (all data)	R_1 = 0.0684, wR_2 = 0.1024	R_1 = 0.2086, wR_2 = 0.2339
$\Delta\rho_{max}$, $\Delta\rho_{min}$ (e Å^{-3})	0.164, −0.102	1.681, −0.574

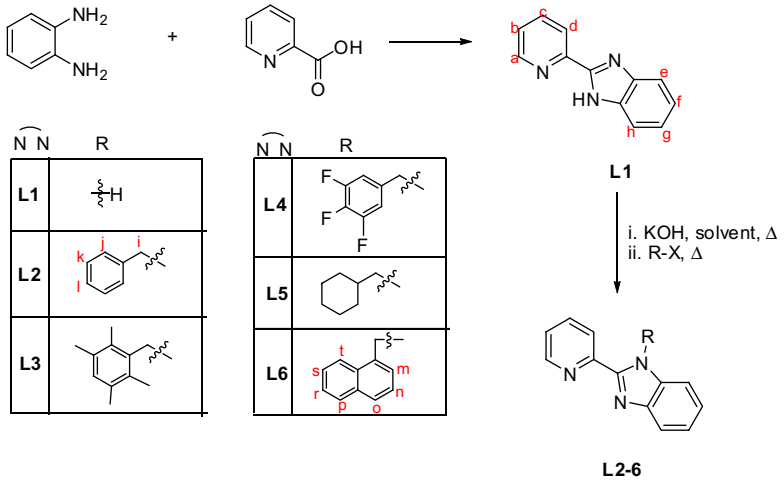

Scheme 1. Synthesis of ligands and numbering scheme for the ligands.

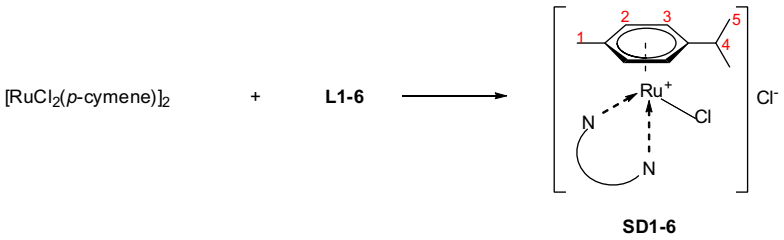

Scheme 2. Synthesis of complexes and numbering scheme for the ligands.

of the H atoms were fixed at $U_{iso}(H) = 1.2U_{eq}$ ($1.5U_{eq}$ for methyl and water) of their parent atoms. In the final difference Fourier map of **SD6**, there are four high maximum residual electron density peaks (1.68, 1.56, 1.55 and 1.43 e/Å^3) which are located 1.18 and 1.06 Å from Ru1A atom and 1.12 and 1.07 Å from Ru1B atom, respectively. Data collection: X-AREA [30], cell refinement: X-AREA, data reduction: X-RED32 [30]. Crystal data, data collection and structure refinement details are summarized in Table 1. The general-purpose crystallographic tool PLATON [31] was used for the structure analysis and presentation of the results. Molecular graphics were generated by using ORTEP-3 [32].

3. Results and discussion

3.1. Synthesis of compounds

In this work, first, **L1** was obtained from the reaction of 2-picolonic acid and *o*-phenylenediamine in the presence of *o*-phosphoric acid. Latter, **L2–6** was synthesized via N-alkylation of **L1** in alkaline solution (Scheme 1). Finally, Ru(II) complexes (**SD1–6**) was obtained between the reaction of $[RuCl_2(p\text{-cymene})]_2$ and ligands (Scheme 2). Synthesized ligands and complexes were soluble in most organic solvents such as alcohol, DCM, acetone. Also, Ru(II) complexes were slightly soluble in H_2O.

3.2. Characterization of compounds

Synthesized compounds were characterized by CHN analysis, FT-IR, UV–Vis and NMR spectroscopies.

Aromatic C–H stretching vibrations are observed at approximately 3000 cm^{-1} in ligands as medium sized peaks except for **L1**. For **L1**, aromatic C–H stretching vibrations are shown as very broad peak between 3200 and 2800 cm^{-1} because of intra-molecular H-bonding. The aliphatic C–H stretching vibrations for $-CH_2$ and $-CH_3$ are monitored in the region of 3000–2900 cm^{-1} for **L2–6** as expected. Additionally, aliphatic C–H stretching vibrations belonging to *p*-cymene group are showed in the region of 3000–2850 cm^{-1} in Ru(II) complexes. The C=N stretching bands appear in the range of 1621–1609 cm^{-1} in the ligands. Under coordination of Ru(II), C=N stretching bands are slightly shifted to a lower wave number. In the FT-IR spectra of Ru(II) complexes, there are a broad

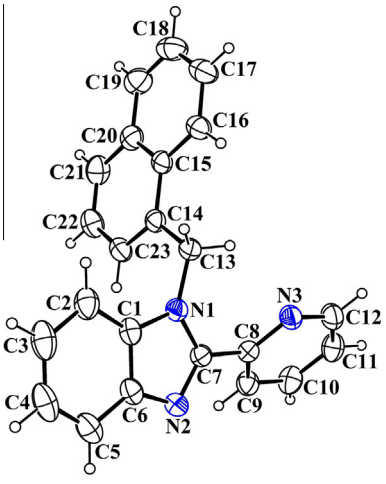

Fig. 1. A view of L6 showing the atom-numbering scheme. Displacement ellipsoids are drawn at the 30% probability level and H atoms are shown as small spheres of arbitrary radii.

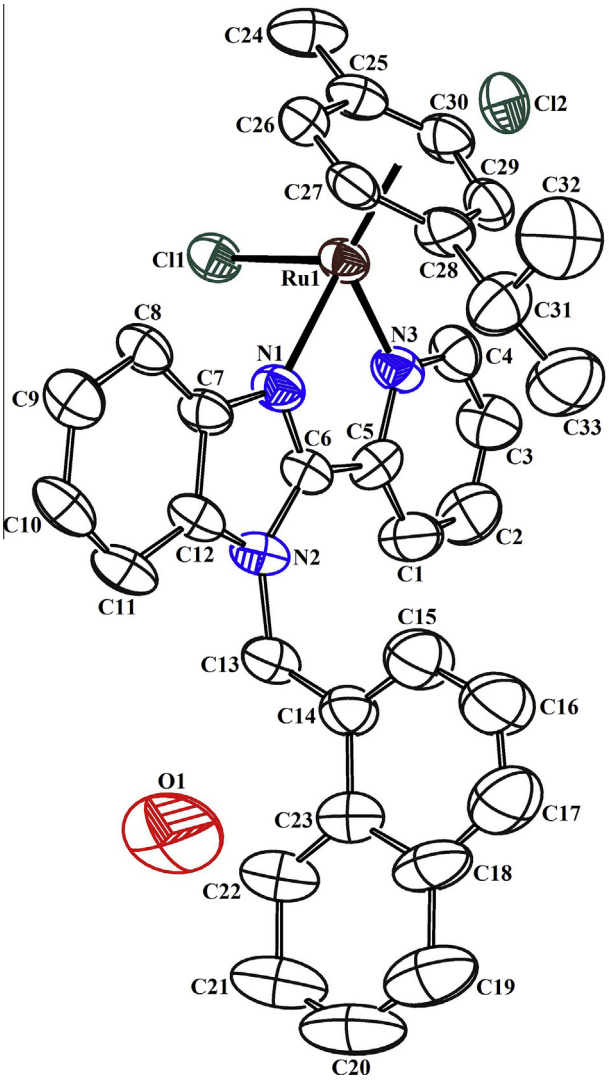

Fig. 2. A view of **SD6** showing the atom-numbering scheme. Displacement ellipsoids are drawn at the 30% probability level. For clarity, H atoms have been omitted.

Table 2
Selected geometric parameters for **L6** and **SD6**.

Parameter	**L6**	Parameter	**SD6**	
			Molecule A	Molecule B
Bond lengths (Å)				
N1–C1	1.3823(14)	Ru1–Cl1	2.399(3)	2.401(3)
N1–C7	1.3753(15)	Ru1–N1	2.059(7)	2.063(8)
N1–C13	1.4595(14)	Ru1–N3	2.059(9)	2.090(8)
N2–C6	1.3841(16)	Ru1–C25	2.231(10)	2.214(12)
N2–C7	1.3155(14)	Ru1–C26	2.184(10)	2.170(10)
N3–C8	1.3399(15)	Ru1–C27	2.137(11)	2.180(11)
N3–C12	1.3331(16)	Ru1–C28	2.144(13)	2.197(14)
C7–C8	1.4768(16)	Ru1–C29	2.137(10)	2.151(10)
C13–C14	1.5056(16)	Ru1–C30	2.211(10)	2.179(11)
		N1–C6	1.310(12)	1.309(11)
		N1–C7	1.396(11)	1.407(10)
		N2–C6	1.380(11)	1.365(11)
		N2–C12	1.395(12)	1.407(11)
		N2–C13	1.473(12)	1.431(11)
		N3–C4	1.393(12)	1.361(11)
		N3–C5	1.363(12)	1.365(12)
		C5–C6	1.487(14)	1.456(12)
		C13–C14	1.492(15)	1.516(13)
Bond angles (°)				
N1–C7–N2	113.23(10)	Cl1–Ru1–N1	86.1(2)	84.1(2)
C1–N1–C7	106.12(9)	Cl1–Ru1–N3	84.4(2)	87.3(2)
C6–N2–C7	104.74(10)	Cl1–Ru1–C25	89.3(3)	88.8(3)
C8–N3–C12	116.68(11)	Cl1–Ru1–C26	96.7(3)	99.6(4)
N1–C1–C2	131.67(12)	Cl1–Ru1–C27	128.3(4)	130.4(4)
N1–C1–C6	105.55(10)	Cl1–Ru1–C28	165.4(3)	168.0(3)
N1–C7–C8	124.49(10)	Cl1–Ru1–C29	144.9(3)	144.2(4)
N1–C13–C14	114.19(9)	Cl1–Ru1–C30	109.6(3)	108.4(4)
N2–C6–C5	130.13(13)	N1–Ru1–N3	75.8(3)	74.8(3)
N2–C6–C1	110.33(10)	N1–Ru1–C25	152.7(4)	148.9(4)
N2–C7–C8	122.28(10)	N1–Ru1–C26	115.3(3)	114.0(4)
N3–C8–C7	117.70(10)	N1–Ru1–C27	95.0(3)	94.1(4)
N3–C8–C9	122.93(11)	N1–Ru1–C28	97.8(3)	98.8(4)
N3–C12–C11	124.26(13)	N1–Ru1–C29	127.3(4)	129.7(5)
		N1–Ru1–C30	164.1(4)	167.4(5)
		N3–Ru1–C25	130.5(4)	135.2(4)
		N3–Ru1–C26	168.8(3)	169.2(3)
		N3–Ru1–C27	145.9(4)	140.0(4)
		N3–Ru1–C28	110.2(4)	104.7(4)
		N3–Ru1–C29	93.0(4)	90.8(4)
		N3–Ru1–C30	102.4(4)	103.1(4)

band approximately between 3500 and 3200 cm^{-1} region because of their hygroscopic nature. This observation is supported by the results of elemental analysis of all complexes and X-ray analysis of **SD6**.

Two strong peaks below 300 nm is assigned to $\pi \rightarrow \pi^*$ and $n \rightarrow \pi^*$ transition in UV–Vis spectra of the ligands. These peaks are slightly red-shifted with the formation of complex and new peak belonging Ru(dπ) $\rightarrow \pi^*$ CT transition is formed.

In the ^{1}H NMR spectra of **L1**, –N*H* proton was observed as singlet at 13.11 ppm. This peak was not appeared for **L2–6** as expected. Other aromatic protons in **L1–4** and **L6** were observed in the range of 6–10 ppm. –*Ha* protons in ligands were monitored in the range of 6.10–6.72 ppm as singlet except for **L5**. These protons were appeared at 4.76 ppm as doublet in **L5**. Under coordination to Ru(II), the peaks of aromatic protons of **L1–6** generally shifted to low field in ^{1}H NMR spectra. Additionally, new peaks belonging to *p*-cymene groups observed in ^{1}H NMR spectra for Ru(II) complexes except **SD1** and **SD4**. –H_4 proton for **SD1** and **SD4** were not observed in ^{1}H NMR spectra because this peak remains under solvent peaks. On the other hand, the ^{13}C NMR spectra are consistent with proposed structures. Detailed assignments were made in experimental section.

3.3. Description of the crystal structures

The solid-state structures of the compounds have been confirmed by single crystal X-ray analysis. The perspective ORTEP-3 views of **L6** and **SD6** with the atomic numbering scheme are depicted in Figs. 1 and 2, respectively, while selected bond lengths and angles are given in Table 2. Both compounds crystallize in the triclinic space group $P\bar{1}$ and there are two molecules in the asymmetric unit of **SD6**, labeled as A and B. For the sake of clarity, only one (molecule A) of the two molecules is shown in Fig. 2. In the following discussion, parameters for molecule B are quoted in square brackets.

The molecule of **L6** is composed of a benzimidazole ring with a naphthalen-1-ylmethyl group and a pyridine ring in the 1- and 2-positions of the benzimidazole, respectively. The benzimidazole and pyridine rings of the molecule do not share a common plane but rather make a dihedral angle of 41.82(6)°. The naphthalene ring is almost perpendicular to both the benzimidazole and pyridine rings with dihedral angles of 86.73(5)° and 85.86(6)°, respectively. Furthermore, the dihedral angle between the five- and six-membered rings of the benzimidazole is 1.76(8)°, while the crossed torsion angles at the junction, *i.e.*, N1–C1–C6–C5 and N2–C6–C1–C2 are 178.67(11)° and 177.32(11)°, respectively. The imine N=C and amine N–C bond distances in the benzimidazole ring [1.3155(14) and 1.3753(15) Å, respectively] are not same, with the 'imine' length shorter than the 'amine' length, as expected. The bond lengths and angles of **L6** present no unusual features.

Cationic complex of **SD6** consists of an **L6** ligand with an Ru(II) metal centre, one *p*-cymene ligand and one Cl ligand. The charge is balanced by a chloride anion and the compound also crystallizes with a water solvent molecule per cationic complex. The complex has the familiar half-sandwich "three-legged piano-stool" geometry with the η^6 π-bound arene ring forming the seat, and the two

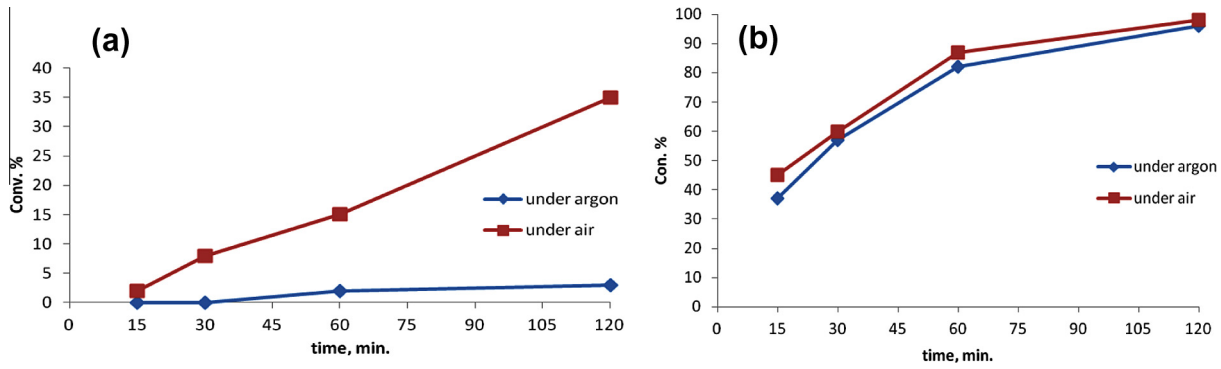

Fig. 3. TH of acetophenone catalyzed with **SD5** in 2-propanol in the presence of KOH (a) S/C/B ratio is 1/0.01/0.01 (b) S/C/B ratio is 1/0.01/4.

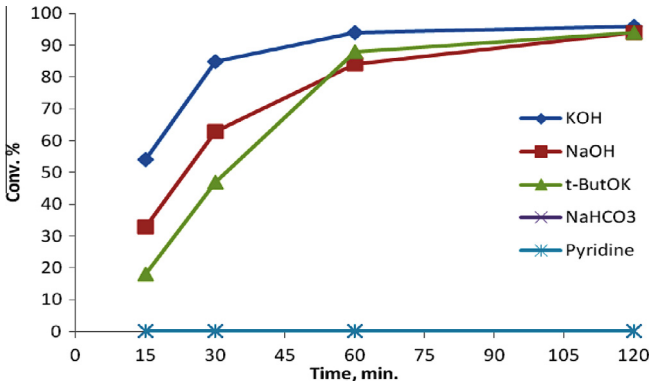

Fig. 4. TH of acetophenone catalyzed with **SD2** in 2-propanol in the presence of different bases (S/C/B ratio is 1/0.01/4).

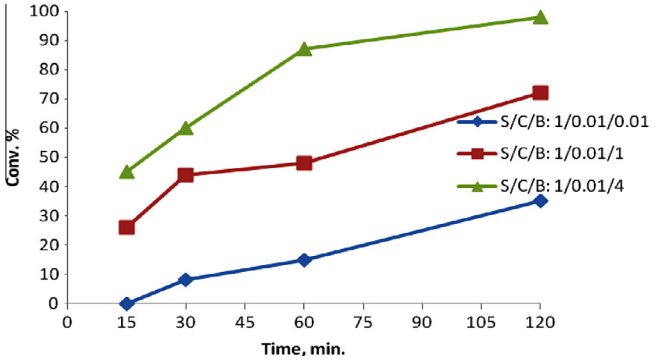

Fig. 5. TH of acetophenone catalyzed with **SD5** in 2-propanol in the presence of different KOH concentrations.

nitrogen atoms of the **L6** ligand and one terminal chloride ligand as the legs of the piano-stool.

The Ru ion exhibits a pseudo-octahedral coordination geometry, with the arene formally occupying three facial coordination sites. However, the coordination geometry around the Ru atom may be regarded as a tetrahedron with considerable trigonal distortion, taking into account the center of the η^6-*p*-cymene aromatic ring as the fourth ligand position. If *X* is defined as the centroid of the aromatic ring, the Ru–*X* distance is found to be 1.6730(8) Å [1.6668(8) Å], and the Cl1–Ru1–*X*, N1–Ru1–*X* and N3–Ru1–*X* angles are 127.53(7)°, 132.8(2)° and 131.8(2)° [129.12(8)°, 132.5(2)° and 130.2(2)°], respectively. The Cl1–Ru1–N1, Cl1–Ru1–N3 and N1–Ru1–N3 angles [mean 82.1(2)° for both molecule A and molecule B] are smaller than the ideal tetrahedral angle (109.47°), which is counterbalanced by the extending of the *X*–Ru–*L* (L is Cl1, N1 or N3) angles [mean 130.7(2)° for molecule A and 130.6(2)° for molecule B].

Similar to related Ru(II)-arene complexes [33–41], there are substantial differences in the C–C [1.352(15)–1.460(14) Å for molecule A and 1.380(15)–1.424(15) Å for molecule B] and Ru–C [2.137(10)–2.231(10) Å for molecule A and 2.151(10)–2.214(12) Å for molecule B] distances for the arene ring. In the complex, the arene ring is planar with an r.m.s deviation from the plane being 0.0152 Å [0.0094Å]. The two N-donor atoms of the bidentate ligand form a five-membered metallacycle (containing atoms Ru1/N1/C6/C5/N3) with an r.m.s deviation from the plane being 0.0283 Å [0.0163Å]. The bond distances of Ru–Cl1, Ru1–N1 and Ru1–N3 are 2.399(3), 2.059(7) and 2.059(9) Å [2.401(3), 2.063(8) and 2.090(8) Å], respectively. When the bond lengths in the coordinated **L6** ligand are compared with those in its free form, it is seen that coordination elongates N2–C6, N3–C8 and N3–C12 bonds, while N2–C7 bond remains almost unchanged. In addition, C6–N2–C7 and C8–N3–C12 angles expand.

Many Ru(II)–arene complexes having the same coordination environment have been reported crystallographically [33–41]. According to the bond lengths in these structures, the Ru–*X*, Ru–C, Ru–Cl and Ru–N bond lengths vary from 1.674 to 1.704 Å, from 2.141 to 2.273 Å, from 2.385 to 2.432 Å and from 2.077 to 2.130 Å, respectively. So, it can be said that the coordination bond distances agree well with the literature values.

3.4. Catalytic properties

Synthesized complexes (**SD1**–**6**) were tested in transfer hydrogenation of acetophenone as catalyst. In a typical catalytic reaction, **SD1**–**6** (0.0085 mmol), KOH (0.85 mmol) and acetophenone (0.85 mmol) was stirred at 82 °C in 2-propanol (4 mL). Reactions were monitored by GC. We investigated optimum reaction conditions and **SD2** and **SD5** were selected as reference catalyst for this purpose. Firstly, acetophenone were transfer hydrogenated via **SD5** in 2-propanol (4 mL) in the presence KOH as a co-catalyst in open

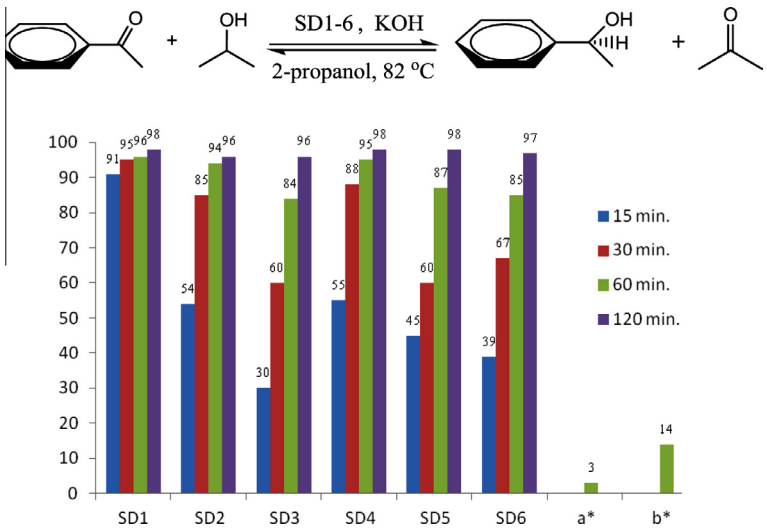

Fig. 6. TH of acetophenone (1 mmol) catalyzed by **SD1**–**6** (0.01 mmol) using KOH (4 mmol) in the presence of 2-propanol (4 mL). a* in the absence of catalyst. b* using [Ru(*p*-cymene)Cl_2]$_2$ as catalyst.

air and under argon atmosphere with different S/C/B ratios. Results showed that open air reactions had good yields (Fig. 3).

Various base types as co-catalyst were tested using **SD2** catalyst (Fig. 4). Results show that KOH has best activity under those conditions. $NaHCO_3$ and pyridine does not show any activity.

Finally, different KOH concentrations were studied for the determination of base amount using **SD5** (Fig. 5). According to Fig. 5, for these type catalysts, the best ratio of S/C/B is 1/0.01/4.

Then, we tested all complexes for TH of acetophenone under these conditions (Fig. 6). The results show that the TH of acetophenone could be achieved with high efficiency for all catalysts (**S1**–**6**).

According to Fig. 6; best result for 1 h was obtained with **SD1**. This observation may be related with NH functionality. It was found that the catalytic activity of the other complexes for the TH of acetophenone follow the order **SD4** > **SD2** > **SD5** > **SD6** > **SD3**, respectively.

4. Conclusion

In this paper, a series of heteroleptic Ru(II) complexes ([RuCl(*p*-cymene)(**L1**–**6**)]Cl; (**SD1**–**6**)) have been synthesized in good yields by the reaction of $[RuCl_2(p\text{-cymene})]_2$ with bidentate **L1**–**6** ligands. One ligand and one complex were structurally characterized with single crystal X-ray diffraction. Synthesized complexes were tested for the transfer hydrogenation of acetophenone with the use of 2-propanol in the presence of KOH under air. Generally, catalytic efficiency seems to depend on the steric parameters of **L2**–**6**. On the other hand, most effective catalyst under worked conditions is **SD1**.

Acknowledgements

We acknowledge Çanakkale Onsekiz Mart University Scientific Research Projects Commission (Project No: FYL-2013-24) for support and the Faculty of Arts and Sciences, Ondokuz Mayıs University, Turkey, for the use of the STOE IPDS II diffractometer (purchased under grant No. F-279 of the University Research Fund).

Appendix A. Supplementary data

CCDC 930498 and 988448 contain the supplementary crystallographic data for the compounds reported in this article. These data can be obtained free of charge via http://www.ccdc.cam.ac.uk/conts/retrieving.html, or from the Cambridge Crystallographic Data Centre, 12 Union Road, Cambridge CB2 1EZ, UK; fax: (+44) 1223-336-033; or e-mail: deposit@ccdc.cam.ac.uk. Supplementary data associated with this article can be found, in the online version, at http://dx.doi.org/10.1016/j.poly.2014.10.012.

References

[1] A. Togni, L.M. Venanzi, Nitrogen donors in organometallic chemistry and homogeneous catalysis, Angew. Chem., Int. Ed. 33 (1994) 497.
[2] L. Ackermann, Carboxylate-assisted ruthenium-catalyzed alkyne annulations by C–H/Het-H bond functionalizations, Acc. Chem. Res. 47 (2014) 281.
[3] A. Bergamo, C. Gaiddon, J.H.M. Schellens, J.H. Beijnen, G. Sava, Approaching tumour therapy beyond platinum drugs Status of the art and perspectives of ruthenium drug candidates, J. Inorg. Biochem. 106 (2012) 90.
[4] P.B. Arockiam, C. Bruneau, P.H. Dixneuf, Ruthenium(II)-catalyzed C–H bond activation and functionalization, Chem. Rev. 112 (2012) 5879.
[5] B.E. Hardin, H.J. Snaith, M.D. McGehee, The renaissance of dye-sensitized solar cells, Nat. Photon. 6 (2012) 162.
[6] S.I. Kozhushkov, L. Ackermann, Ruthenium-catalyzed direct oxidative alkenylation of arenes through twofold C–H bond functionalization, Chem. Sci. 4 (2013) 886.
[7] R.D. Costa, E. Orti, H.J. Bolink, F. Monti, G. Accorsi, N. Armaroli, Luminescent ionic transition-metal complexes for light-emitting electrochemical cells, Angew. Chem., Int. Ed. 51 (2012) 8178.
[8] M.R. Gill, J.A. Thomas, Ruthenium(II) polypyridyl complexes and DNA-from structural probes to cellular imaging and therapeutics, Chem. Soc. Rev. 41 (2012) 3179.
[9] S. Dayan, N. Kayaci, N.O. Kalaycioglu, O. Dayan, E.C. Ozturk, Synthesis of ruthenium(II) complexes derived from reduced imine ligands: As catalysts for transfer hydrogenation of ketones, Inorg. Chim. Acta 401 (2013) 107.
[10] O. Kohle, S. Ruile, M. Gratzel, Ruthenium(II) charge-transfer sensitizers containing 4,4′-dicarboxy-2,2′-bipyridine. Synthesis, properties, and bonding mode of coordinated thio- and selenocyanates, Inorg. Chem. 35 (1996) 4779.
[11] M.K. Nazeeruddin, E. Muller, R. Humphry-Baker, N. Vlachopoulos, M. Gratzel, Redox regulation in ruthenium(II) polypyridyl complexes and their application in solar energy conversion, J. Chem. Soc., Dalton Trans. (1997) 4571.
[12] M.A. Haga, K. Wang, N. Kato, H. Monjushiro, Electrochemical properties of dinuclear Ru complex Langmuir–Blodgett films towards molecular electronics, Mol. Cryst. Liq. Crys. A 337 (1999) 89.
[13] V.G. Vaidyanathan, B.U. Nair, Synthesis, characterization and DNA binding studies of a ruthenium(II) complex, J. Inorg. Biochem. 91 (2002) 405.
[14] M. Haga, T. Takasugi, A. Tomie, M. Ishizuya, T. Yamada, M.D. Hossain, M. Inoue, Molecular design of a proton-induced molecular switch based on rod-shaped Ru dinuclear complexes with bis-tridentate 2,6-bis(benzimidazol-2-yl) pyridine derivatives, Dalton Trans. (2003) 2069.
[15] A. Singh, B. Chetia, S.M. Mobin, G. Das, P.K. Iyer, B. Mondal, Ruthenium monoterpyridine complexes with 2,6-bis(benzimidazol-2-yl)pyridine: Synthesis, spectral properties and structure, Polyhedron 27 (2008) 1983.
[16] J.J. Concepcion, J.W. Jurss, P.G. Hoertz, T.J. Meyer, Catalytic and surface-electrocatalytic water oxidation by redox mediator-catalyst assemblies, Angew. Chem., Int. Ed. 48 (2009) 9473.
[17] C. Bhaumik, S. Das, D. Saha, S. Dutta, S. Baitalik, Synthesis, characterization, photophysical, and anion-binding studies of luminescent heteroleptic bis-tridentate ruthenium(II) complexes based on 2,6-bis(benzimidazole-2-yl)pyridine and 4′-substituted 2,2′:6′,2″ terpyridine derivatives, Inorg. Chem. 49 (2010) 5049.
[18] O. Dayan, F. Dogan, I. Kaya, B. Cetinkaya, Palladium(II) complexes containing 2,6-bis(imino)pyridines: Synthesis, characterization, thermal study, and catalytic activity in Suzuki reactions, Synth. React. Inorg. Met. Org. Chem. 40 (2010) 337.
[19] R. Noyori, S. Hashiguchi, Asymmetric transfer hydrogenation catalyzed by chiral ruthenium complexes, Acc. Chem. Res. 30 (1997) 97.
[20] (a) B. Stefane, F. Pozgan, Advances in catalyst systems for the asymmetric hydrogenation and transfer hydrogenation of ketones, Catal. Rev. 56 (2014) 82;
(b) J.-I. Ito, H. Nishiyama, Recent topics of transfer hydrogenation, Tetrahedron Lett. 55 (2014) 3133.
[21] S. Gunnaz, N. Ozdemir, S. Dayan, O. Dayan, B. Cetinkaya, Synthesis of ruthenium(II) complexes containing tridentate triamine ('(NNN)over-cap') and bidentate diamine ligands ((NN)over-cap'): as catalysts for transfer hydrogenation of ketones, Organometallics 30 (2011) 4165.
[22] O. Dayan, N. Ozdemir, Z. Serbetci, M. Dincer, B. Cetinkaya, O. Buyukgungor, Synthesis and catalytic activity of ruthenium(II) complexes containing pyridine-based tridentate triamines ('NNN') and pyridine carboxylate ligands (NO), Inorg. Chim. Acta 392 (2012) 246.
[23] O. Dayan, S. Dayan, I. Kani, B. Cetinkaya, Ruthenium(II) complexes bearing pyridine-based tridentate and bidentate ligands: catalytic activity for transfer hydrogenation of aryl ketones, Appl. Organomet. Chem. 26 (2012) 663.
[24] M.A. Bennett, T.N. Huang, T.W. Matheson, A.K. Smith, (Eta-6-hexamethylbenzene)ruthenium complexes, Inorg. Synth. 21 (1982) 74.
[25] A.K. Dutta, S.K. Maji, S. Dutta, C.R. Lucas, B. Adhikary, Syntheses, crystal structure, spectroscopic, redox and magnetic properties of oxo- and carboxylato-bridged polynuclear iron(III) complexes with phenolate- and pyridine-substituted benzimidazole ligands, Polyhedron 44 (2012) 34.
[26] W.K. Huang, C.W. Cheng, S.M. Chang, Y.P. Lee, E.W.G. Diau, Synthesis and electron-transfer properties of benzimidazole-functionalized ruthenium complexes for highly efficient dye-sensitized solar cells, Chem. Commun. 46 (2010) 8992.
[27] N.M. Shavaleev, Z.R. Bell, T.L. Easun, R. Rutkaite, L. Swanson, M.D. Ward, Complexes of substituted derivatives of 2-(2-pyridyl)benzimidazole with Re(I), Ru(II) and Pt(II): structures, redox and luminescence properties, Dalton Trans. (2004) 3678.
[28] G.M. Sheldrick, A short history of SHELX, Acta Crystallogr., Sect. A 64 (2008) 112.
[29] L.J. Farrugia, WinGX and ORTEP for Windows: an update, J. Appl. Crystallogr. 45 (2012) 849.
[30] Stoe & Cie, X-AREA (Version 1.18) and X-RED32 (Version 1.04); Stoe & Cie, Darmstadt, Germany, 2002.
[31] A.L. Spek, Structure validation in chemical crystallography, Acta Crystallogr., Sect. D 65 (2009) 148.
[32] L. Farrugia, ORTEP-3 for windows – A version of ORTEP-III with a graphical user interface (GUI), J. Appl. Crystallogr. 30 (1997) 565.
[33] H. Ben Ammar, J. Le Notre, M. Salem, M.T. Kaddachi, L. Toupet, J.L. Renaud, C. Bruneau, P.H. Dixneuf, New [Ru-3(CO)(12)]-based catalysts with imidazolinium salt, diimine, or bis(oxazoline) ligands and ruthenium bis(oxazoline) complex for tandem isomerisation/claisen rearrangement of dienyl ethers - X-ray structure of [RuCl{(R, R)-bis(isopropyloxazoline)}(p-cymene)]BF4, Eur. J. Inorg. Chem. (2003) 4055.
[34] D.L. Davies, J. Fawcett, S.A. Garratt, D.R. Russell, (Arene)ruthenium complexes with bis(oxazolines): Synthesis and applications as asymmetric catalysts for Diels–Alder reactions, Organometallics 20 (2001) 3029.

[35] J.W. Faller, A. Lavoie, Highly enantioselective Diels–Alder catalysis with a chiral ruthenium bisoxazoline complex, J. Organomet. Chem. 630 (2001) 17.
[36] R. Lalrempuia, M.R. Kollipara, Reactivity studies of eta(6)-arene ruthenium (II) dimers with polypyridyl ligands: Isolation of mono, binuclear p-cymene ruthenium (II) complexes and bisterpyridine ruthenium (II) complexes, Polyhedron 22 (2003) 3155.
[37] W.B. Yao, K. Kavallieratos, S. de Gala, R.H. Crabtree, Dipyrimidylamine and tripyrimidylamine as chelating N-donor ligands, Inorg. Chim. Acta 311 (2000) 45.
[38] J.X. Ong, C.W. Yap, W.H. Ang, Rational design of selective organoruthenium inhibitors of protein tyrosine phosphatase 1B, Inorg. Chem. 51 (2012) 12483.
[39] K.C. Cheung, W.L. Wong, M.H. So, Z.Y. Zhou, S.C. Yan, K.Y. Wong, A dinuclear ruthenium catalyst with a confined cavity: selectivity in the addition of aliphatic carboxylic acids to phenylacetylene, Chem. Commun. 49 (2013) 710.
[40] C.A. Vock, C. Scolaro, A.D. Phillips, R. Scopelliti, G. Sava, P.J. Dyson, Synthesis, characterization, and in vitro evaluation of novel ruthenium(II) eta(6)-arene imidazole complexes, J. Med. Chem. 49 (2006) 5552.
[41] R.R. Dykeman, K.L. Luska, M.E. Thibault, M.D. Jones, M. Schlaf, M. Khanfar, N.J. Taylor, J.F. Britten, L. Harrington, Catalytic deoxygenation of terminal-diols under acidic aqueous conditions by the ruthenium complexes [(eta(6)-arene) Ru(X)(N boolean AND N)](OTf)(n), X = H2O, H, eta(6)-arene = p-Me-Pr-i-C6H4, C6Me6, N boolean AND N = bipy, phen, 6,6 '-diamino-bipy, 2,9-diamino-phen, n = 1, 2) Influence of the ortho-amine substituents on catalytic activity, J. Mol. Catal. A Chem. 277 (2007) 233.